

and a maximum coordination number of six. Similarly in solid fluoro complex salts, the positive metal ions or hydrogen bonding  $\text{NH}_4^+$  ion probably interact sufficiently strongly with the small nonpolarizable  $\text{F}^-$  ions in the crystals to pull them further away from the  $\text{An(IV)}$  ions allowing high coordination numbers. With very large, low charge density ions such as  $(\text{C}_2\text{H}_5)_4\text{N}^+$  such an effect would be much weaker, and the lower coordination number  $\text{AnF}_6^{2-}$  ions are stable relative to higher coordination number arrangements.

Finally, it should be noted that extraction of hydrated  $\text{UF}_4$  from water suspension into tridecyl- and tetradecyl-ammonium fluoride in low dielectric solvents has been reported,<sup>27</sup> and it was claimed without any real evidence that

(27) A. A. Lipovski and S. A. Nikitina, *Radiokhimiya*, 11, 44 (1969).

the  $\text{UF}_6^{2-}$  ion was the species present in the water-saturated organic phase. That this claim is not correct is demonstrated by the fact that the reported absorption spectra of the solutions are not at all similar to that of  $\text{UF}_6^{2-}$  shown here and by the fact that the values reported for  $\epsilon_{\text{max}}$  between 560 and 700 nm vary from 8 to 16 whereas that for  $\text{UF}_6^{2-}$  is 0.85.

**Acknowledgments.** The authors express their appreciation to C. E. Plucinski and R. J. Sironen for analytical assistance and to R. S. Cichorz who measured the ir spectrum of  $[(\text{C}_2\text{H}_5)_4\text{N}]_2\text{PuF}_6$ .

**Registry No.**  $[(\text{C}_2\text{H}_5)_4\text{N}]_2\text{UF}_6$ , 42294-80-4;  $[(\text{C}_2\text{H}_5)_4\text{N}]_2\text{PuF}_6$ , 42294-81-5;  $[(\text{C}_2\text{H}_5)_4\text{N}]_2\text{NpF}_6$ , 42294-82-6.

Contribution from Brookhaven National Laboratory, Upton, New York 11973

## Formation and Properties of Iron Titanium Hydride<sup>1</sup>

J. J. REILLY\* and R. H. WISWALL, Jr.

Received March 1, 1973

The intermetallic compound FeTi reacts directly with hydrogen to form, in succession, hydrides of the approximate compositions  $\text{FeTiH}$  and  $\text{FeTiH}_2$ . The composition limits have been determined and are diagrammed. Both hydrides have dissociation pressures of over 1 atm at  $0^\circ$ , unlike the very stable  $\text{TiH}_2$ . The relative partial molar enthalpies of hydrogen have the rather low values of  $-3.36$  kcal/g-atom of hydrogen in the lower hydride and  $-3.70$  to  $-4.03$  in the higher; the properties of the latter vary with the hydrogen content. Pronounced hysteresis effects are observed, the absorption isotherms of pressure vs. composition frequently being several atmospheres higher, at a given composition, than the desorption isotherms. The lower hydride,  $\text{FeTiH}$ , has tetragonal symmetry and a density of  $5.88$  g/cm<sup>3</sup>. The higher hydride has a cubic structure and a density of  $5.47$  g/cm<sup>3</sup> ( $\text{FeTiH}_{1.93}$ ). The hydriding behavior is quite sensitive to the composition of the solid phase. If Ti is in slight excess over the equiatomic proportion, the pressure-composition isotherms no longer exhibit the plateaus and inflections characteristic of the appearance of new phases.

Iron and titanium form two known stable intermetallic compounds,  $\text{FeTi}$  and  $\text{Fe}_2\text{Ti}$ .<sup>2</sup> It is also generally accepted that a third compound,  $\text{FeTi}_2$ , exists above  $1000^\circ$ , decomposing to  $\text{FeTi}$  and  $\text{Ti}$  below that temperature.<sup>3</sup> We have briefly noted previously<sup>4</sup> that one of these compounds,  $\text{FeTi}$ , will react directly with hydrogen to form an easily decomposed hydride which may be useful as a hydrogen storage medium. Our purpose here is to discuss the Fe-Ti-H system in some detail with particular emphasis on the reaction of  $\text{FeTi}$  with hydrogen and the formation and properties of two ternary hydrides,  $\text{FeTiH}_{\sim 1}$  and  $\text{FeTiH}_{\sim 2}$ .

### Experimental Section

The Fe-Ti alloys were prepared from zone-refined Fe and Ti in an arc furnace under an argon atmosphere, although it should be noted that no significant differences were observed when commercial grade Fe and Ti were substituted for the zone-refined starting material. Initially we had prepared the alloys in an induction furnace; however, it appeared that the resulting products were contaminated by the

alumina crucible material, which had an inhibiting effect upon their reaction with hydrogen. Contamination of iron titanium alloys by alumina crucibles has been noted previously.<sup>2</sup> All the alloys were quite brittle and all samples were crushed to pass through a 10-mesh screen. It was not necessary to carry out the crushing step in an inert atmosphere. The samples, weighing  $\sim 10$  g, were introduced into a high-pressure hydriding reactor, the construction of which has been previously discussed in detail.<sup>5</sup>

Our procedure for hydriding metals which form unstable hydrides, as in this instance, has also been described,<sup>6</sup> and only a brief synopsis will be given here. The reactor was loaded with the granular alloy samples, sealed, evacuated, and then heated to  $400$ – $450^\circ$  while outgassing continuously. Upon reaching the cited temperature range, hydrogen was admitted to the reactor until the pressure was  $\sim 7$  atm. There was usually a slight drop in hydrogen pressure at this point due to some solution of hydrogen in the metal phase. After  $\sim 30$  min the reactor was evacuated and cooled to room temperature at which point  $\text{H}_2$  was admitted to the reactor until the pressure was  $\sim 65$  atm. Usually the metal-hydrogen reaction proceeded immediately with the evolution of heat. If no reaction took place over a 15-min period, the above procedure was repeated. It should be noted that if the alloy is in ingot form, rather than granular, the initiation of the reaction is somewhat more difficult and may require several such treatments. In order to obtain a highly active metal substrate, the sample was hydrided and dehydrided several times. Dehydriding was accomplished by outgassing and heating to  $\sim 200^\circ$ .

The procedure for obtaining the pressure-composition isotherms presented here is essentially the same as that described previously.<sup>5,6</sup> Briefly, it consisted of equilibrating the metal hydride with hydrogen

(1) This work was performed under the auspices of the U. S. Atomic Energy Commission and was also partially supported by U. S. Army Mobility Equipment Research and Development Center, Ft. Belvoir, Va.

(2) R. P. Elliott, "Constitution of Binary Alloys, First Supplement," McGraw-Hill, New York, N. Y., 1965.

(3) D. H. Polonis and J. G. Parr, *Trans. AIME*, 200, 1148 (1954).

(4) (a) K. C. Hoffman, *et al.*, paper presented at the International Automotive Engineering Congress, Society of Automotive Engineers, Detroit, Jan 1969; (b) R. H. Wiswall, Jr., and J. J. Reilly, paper presented at the Intersociety Energy Conversion Engineering Conference, San Diego, Calif., Sept 1972.

(5) J. J. Reilly and R. H. Wiswall, Jr., *Inorg. Chem.*, 6, 2220 (1967).

(6) J. J. Reilly and R. H. Wiswall, Jr., *Inorg. Chem.*, 9, 1678 (1970).

at ~65 atm pressure and at a predetermined temperature. Hydrogen was then withdrawn in a measured amount from the system by venting to an evacuated reservoir of known volume. After equilibrium was reestablished as determined by no further pressure change over a period of ~3 hr, a further aliquot of hydrogen was withdrawn. This step was repeated in succession until the equilibrium pressure was below 1 atm, after which the sample was heated to  $>400^\circ$  and any further hydrogen that evolved was measured. Finally, the sample was cooled to room temperature, removed from the reactor, and analyzed for Fe, Ti, and residual hydrogen. The analysis for the metals was accurate to  $\pm 0.5\%$  and total cumulative error for hydrogen was estimated to be  $\pm 2.5\%$ . Occasionally, the reverse procedure was followed in order to determine hysteresis effects. In these runs, the starting material was an alloy sample that had been activated by previous hydriding and dehydriding; and the points on the pressure vs. composition curve were obtained by adding successive small increments of hydrogen.

All the X-ray data were obtained using a 114.59-mm diameter Norelco powder camera (Debye-Scherrer type) using  $\text{Cu K}\alpha$  or  $\text{Co K}\alpha$  radiation.

### Results and Discussion

The Fe-Ti-H system was explored between the approximate limits, by weight, of 70% Fe-30% Ti and 37% Fe-63% Ti, corresponding to the atomic proportions  $\text{Fe}_2\text{Ti}$  and  $\text{FeTi}_2$ . At the iron-rich end of this range no hydrogen was absorbed, but all compositions richer in Ti than  $\text{Fe}_2\text{Ti}$  did take up hydrogen to some extent. The stable intermetallic compound, FeTi, reacted readily, and a series of pressure-composition isotherms for the FeTi-H system is shown in Figure 1. The composition of the unhydrided alloy, as determined by analysis, was 53.6% Fe and 46.7% Ti. The only metal phase present should be that of FeTi, which was confirmed by an X-ray diffraction pattern taken of the sample. In the graphs the equilibrium dissociation pressure of the hydride is plotted against the hydrogen content of the alloy expressed as the ratio of hydrogen atoms to the total number of metal atoms ( $\text{H}/(\text{Fe} + \text{Ti})$  or simply  $\text{H}/\text{M}$ ). The shape of the isotherms can be interpreted as follows: on the left, where the isotherms rise steeply as the hydrogen content of solid increases, is the region of solid solution of hydrogen in the Fe-Ti metal lattice. This solid solubility region may be designated as the  $\alpha$  phase of the FeTi-H system. As the hydrogen content of the solid is further increased, the equilibrium pressure remains constant and forms, so to speak, a plateau. The composition at which the plateau begins marks the point at which a new phase appears and also marks the maximum solubility of hydrogen in the  $\alpha$  phase. At room temperature that composition corresponds to  $\text{FeTiH}_{0.10}$  ( $\text{H}/\text{M} = 0.05$ ). The new phase is the monohydride or  $\beta$  phase of the FeTi-H system. Both the  $\alpha$  and  $\beta$  phases coexist until the solid composition corresponds to  $\text{FeTiH}_{1.04}$  where the isotherms begin a steep ascent. At this point the  $\alpha$  phase had disappeared. The dip shown in the lower temperature isotherms near this composition is discussed below. As the hydrogen content of the  $\beta$  phase is increased, a new phase appears, the  $\gamma$  or dihydride phase. Its exact point of inception is temperature dependent and is somewhat difficult to determine since the upper plateaus are narrow and the breaks in the isotherms quite gradual. The  $55^\circ$  isotherm shows only a vestigial plateau structure and it appears that this temperature is quite close to the critical temperature, above which two discrete solid hydride phases cannot coexist and the monohydride is transformed continuously into the dihydride phase. The  $70^\circ$  isotherm shows no evidence of a plateau in this region.

The effect of hysteresis in the FeTi-H system at  $40^\circ$  is illustrated in Figure 2. It is worth noting that the system almost forms two loops since hysteresis, as would be expected, is substantially reduced in the intermediate single ( $\beta$ ) phase region. The loops do not quite close, perhaps because the

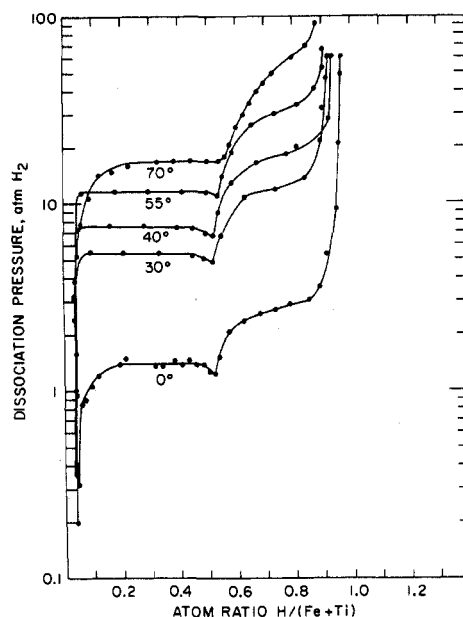


Figure 1. Pressure-composition isotherm for the FeTi-H system. The initial alloy composition was 53.6% Fe and 46.7% Ti.

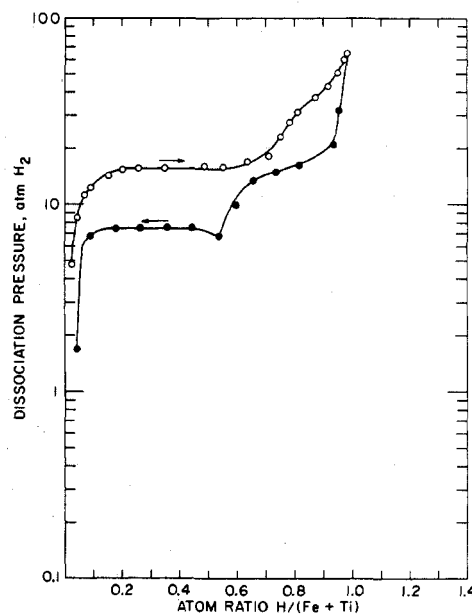


Figure 2. Hysteresis in the FeTi-H system ( $40^\circ$ ).

composition range over which only the  $\beta$  phase is present is quite narrow. As the  $\gamma$  phase appears, hysteresis again increases. It is also of interest to point out that the dip occurring in the lower temperature desorption isotherms at  $\text{H}/\text{M} = 0.5$  does not occur in the absorption isotherm. This situation appears to be analogous to that occurring in the uranium-hydrogen system below  $400^\circ$ , where a similar dip in the desorption isotherm was noted by Spedding, *et al.*,<sup>7</sup> and by Wicke and Otto.<sup>8</sup> Our results indicate that at higher temperatures the dip is less pronounced and finally disappears altogether in the  $70^\circ$  isotherm. This behavior is, again, similar to that of the uranium-hydrogen system, where Libowitz and Gibb<sup>9</sup> found no dips in isotherms determined at high temperatures ( $450^\circ +$ ). Wicke and Otto have suggested that

(7) F. H. Spedding, *et al.*, *Nucleonics*, 4, 4 (1949).

(8) E. Wicke and K. Otto, *Z. Phys. Chem. (Frankfurt am Main)*, 31, 222 (1962).

(9) G. G. Libowitz and T. R. P. Gibb, *J. Phys. Chem.*, 61, 793 (1957).

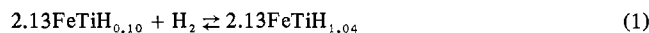
Table I. Relative Partial Molal Quantities Per Gram-Atom of Hydrogen

Compn	$(\bar{H}_H - 1/2H_{H_2}^\circ)$ , $(\bar{S}_H - 1/2S_{H_2}^\circ)$ , $(F_H - 1/2F_{H_2}^\circ)$ ,			$A^a$	$B^a$
	kcal	eu	kcal		
FeTiH <sub>0.1</sub> -FeTiH <sub>1.04</sub>	-3.36	-12.7	+0.42	-3383	+12.7612
FeTiH <sub>1.20</sub>	-3.70	-14.4	+0.57	-3728	+14.4327
FeTiH <sub>1.40</sub>	-3.98	-15.6	+0.65	-4020	+15.6610
FeTiH <sub>1.60</sub>	-4.03	-15.8	+0.68	-4057	+15.9165

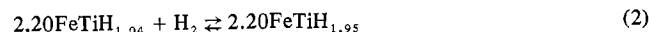
<sup>a</sup> Constants in the equation  $\ln P_{\text{atm}} = (A/T) + B$ .

the phenomenon is due to the supersaturation of hydrogen vacancies in the hydride phase and the fact that the dip is encountered only in desorption isotherms lends support to this explanation.

The reaction taking place in the lower plateau region ( $H/M = 0.10$  to  $H/M = 0.52$ ) can be written as



which is followed by



The variation of the log of the equilibrium dissociation pressure with the reciprocal temperature for several solid compositions is shown in Figure 3. The relationship is linear and obeys the van't Hoff equation in the form of  $\ln P = (A/T) + B$  where  $A$  and  $B$  are constants and  $T$  is the absolute temperature. Thermodynamic values for the iron titanium-hydrogen system were derived from these data and are shown in Table I. They are given as relative partial molal quantities ( $\bar{X}_H - 1/2X_{H_2}^\circ$ ) where  $\bar{X}_H$  is the partial molal enthalpy (entropy or free energy) of hydrogen (as atoms) in the solid, and  $X_{H_2}^\circ$  refers to hydrogen in its standard state as a pure, diatomic ideal gas at a pressure of 1 atm.

The products of reactions 1 and 2 are gray metallike solids, essentially not different in appearance from the granular starting alloy. They are very brittle but are not pyrophoric in air; on the contrary, exposure of these materials to air tends to deactivate them and, even though both hydrides have dissociation pressures appreciably above 1 atm at 25°, they will decompose (*i.e.*, evolve hydrogen) only very slowly in air. Once exposed to air they may be reactivated by repeating the procedure described in the Experimental Section, but a precautionary note should be added here; the remaining hydrided material, though apparently inert, will decompose rapidly into H<sub>2</sub> and FeTi as elevated temperatures are reached (200–300°). Thus the material should not be heated to such temperatures in closed systems unless the free volume is sufficient to accommodate the evolved hydrogen without the buildup of excessive pressure.

As was noted above, iron titanium hydride becomes deactivated upon exposure to air. This property was exploited so that X-ray diffraction patterns of a number of hydride samples could be obtained at 1 atm pressure and room temperature using ordinary powder diffraction techniques and equipment. In order to obtain a suitable sample, iron titanium hydride was prepared in the usual manner. The reactor was then cooled to -196° and evacuated to remove gaseous hydrogen. Air was admitted into the reactor after which it was immediately warmed to room temperature. The reactor was disassembled and a sample for X-ray analysis was taken. The remainder, which was the bulk of the material, was analyzed for hydrogen content by heating it and collecting the evolved hydrogen. If a less than fully hydrided sample was desired, the dihydride was prepared as outlined, but at room temperature (25°) a measured amount of hydrogen was removed from the system to give a sample of the approximate composition desired. The hydride was permitted to reequili-

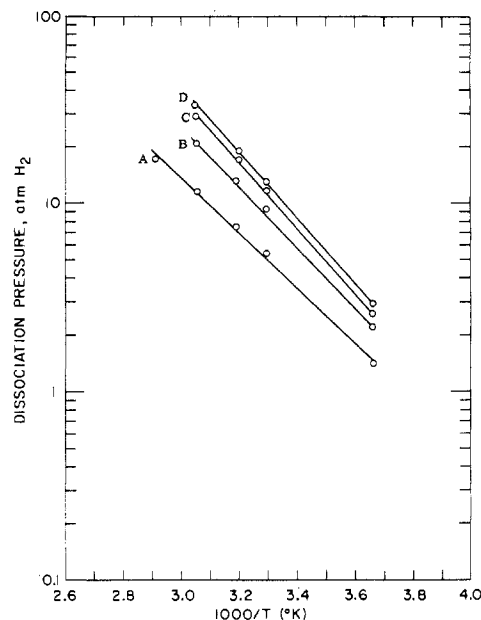


Figure 3. Equilibrium dissociation pressure vs. reciprocal temperature for FeTiH<sub>x</sub>: (A) FeTiH<sub>0.1</sub>-FeTiH<sub>1</sub>; (B) FeTiH<sub>1.2</sub>; (C) FeTiH<sub>1.4</sub>; (D) FeTiH<sub>1.6</sub>.

brate at 25° and then was treated as above. Following this procedure we have been able to obtain X-ray diffraction patterns of a number of hydrided samples whose measured compositions ranged from FeTiH<sub>0.106</sub> to FeTiH<sub>1.93</sub>.

The existence of FeTiH<sub>1</sub> was strongly supported by evidence gathered from an examination of the diffraction pattern of a sample whose composition corresponded to FeTiH<sub>1.06</sub>. The pattern was indexed as having tetragonal symmetry with  $a = 3.18 \text{ \AA}$  and  $c = 8.73 \text{ \AA}$ , thus giving a  $c/a$  ratio of 2.74. There were no reflections present that could be attributed to the FeTi ( $\alpha$ ) phase. The observed and calculated  $d$  spacings are given in Table II. It will be noted in the table that reflections 4 and 5 also appear weakly in the dihydride pattern (discussed below). However, since there are no reflections present which are strong in the latter pattern, the absence of the dihydride may be assumed and both reflections 4 and 5 have been attributed to the monohydride phase. In addition, reflection 5 is fairly strong in the monohydride pattern but weak in the dihydride pattern; further evidence that its placement is correct and proper.

The density of a hydrided sample having composition corresponding to FeTiH<sub>0.80</sub> was measured under benzene and found to be 6.003 g/cm<sup>3</sup>. Since this is a mixture of two phases, hydrogen-saturated FeTi and FeTiH<sub>1</sub>, and if we take the density of the former as 6.50 g/cm<sup>3</sup> (the known density of FeTi), the density of the latter is calculated to be 5.88 g/cm<sup>3</sup>. Knowing the density and using the lattice parameters given above, the number of molecules in a unit cell is calculated to be 2.99 or 3. That the calculated value is so very close to an integral number is substantial evidence that the indexing treatment is correct.

Table II.  $d$  Spacings for FeTiH<sub>1.93</sub><sup>a</sup>

Line no.	Rel intens <sup>b</sup>	$d(\text{obsd})$ , Å	$d(\text{calcd})$ , Å	$hkl$
1	40	2.249	2.249	110
2	20	2.183	2.183	004
3	100	2.145	2.147	103
4	10	1.995	1.999	112
5	50	1.567	1.564	201
6	20	1.284	1.284	204
7	20	1.255	1.247	007

<sup>a</sup> Tetragonal;  $a = 3.18$  Å,  $c = 8.73$  Å. <sup>b</sup> By visual inspection.

The dihydride phase was also indexed and was found to have a cubic structure. The indexed pattern was obtained using a sample whose composition corresponded to FeTiH<sub>1.93</sub>. For this composition the lattice constant  $a$  was found to be 6.61 Å (since this compound is quite nonstoichiometric, the lattice constant is likely to change slightly with hydrogen content). Several of the reflections were very weak and long exposures (~24 hr) were required to define them. It was necessary to use Co K $\alpha$  radiation, since Cu K $\alpha$  gives an appreciable amount of fluorescent radiation with iron-containing materials which results in a background on the film against which weak reflections are difficult to detect and measure. The observed and calculated  $d$  spacings for the dihydride phase are shown in Table III. As discussed above, reflections 4 and 6 also appear in the monohydride pattern, but since there is no other evidence of the presence of the monohydride phase, they have been considered to be a genuine part of the dihydride pattern. The density of FeTiH<sub>1.93</sub>, as measured under benzene, was determined to be 5.47 g/cm<sup>3</sup>; using this value and lattice constant quoted the number of molecules per unit cell was calculated to be 9.00.

From data abstracted from the pressure-composition isotherms discussed above and by using the X-ray diffraction study as ancillary but confirming evidence, a phase diagram of the FeTi-H system has been constructed and is illustrated in Figure 4. The boundaries of the  $\alpha$ - $\beta$  mixed-phase region are fairly well delineated by the pressure-composition isotherms and confirmed broadly by the X-ray data. Unfortunately, the boundaries of  $\beta$ - $\gamma$  region are not so well defined by the pressure-composition data because of the more gradual discontinuities in the isotherms in this composition region. Though carried out only at room temperature, the X-ray data do reflect the phase relationships indicated by the isotherms and add a welcome measure of confidence regarding the location of the phase boundaries for the  $\beta$ - $\gamma$  region.

The FeTi phase is homogeneous in the composition region extending from 45.9% Ti to 48.2% Ti.<sup>10</sup> The equiatomic composition is 46.17% Ti; thus an appreciable amount of Ti can be dissolved in the intermetallic phase. This fact may be responsible for the behavior illustrated in Figure 5, in which the starting alloy was enriched in Ti to the extent that its initial composition, 49.3% Ti and 50.7% Fe, was slightly above that corresponding to the single-phase region. The isotherm B has been significantly distorted, the equilibrium dissociation pressure markedly decreased, and the boundary between the lower and higher hydride is almost indistinguishable. Such a situation is not without precedent and a somewhat similar effect occurs in the LaNi<sub>5</sub>-hydrogen system when excess nickel is added to the starting alloy;<sup>11</sup> *i.e.*, the dissociation pressure of the hydride is increased by a factor

Table III.  $d$  Spacings for FeTiH<sub>1.93</sub><sup>a</sup>

Line no.	Rel intens <sup>b</sup>	$d(\text{obsd})$ , Å	$d(\text{calcd})$ , Å	$hkl$
1	80	2.320	2.337	220
2	100	2.194	2.203	{ 300 221
3	50	2.091	2.090	310
4	10	1.994	1.993	311
5	15	1.755	1.766	321
6	10	1.562	1.558	{ 411 330
7	15	1.416	1.409	332
8	20	1.344	1.349	422
9	10	1.268	1.272	{ 511 333
10	15	1.210	1.207	521
11	10	1.168	1.168	440
12	10	1.104	1.102	{ 600 442

<sup>a</sup> Cubic;  $a = 6.61$  Å. <sup>b</sup> By visual inspection.

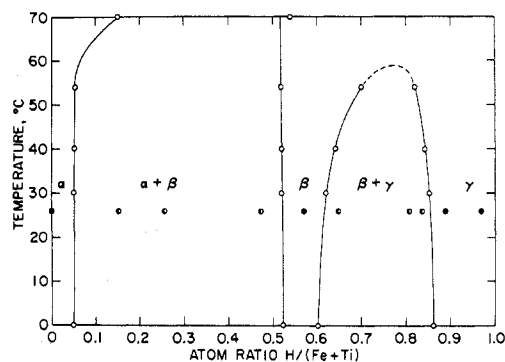


Figure 4. Phase diagram of the FeTi-H system as derived from pressure-composition data. X-Ray diffraction patterns taken at compositions indicated: ●, one solid phase, ○, two solid phases.

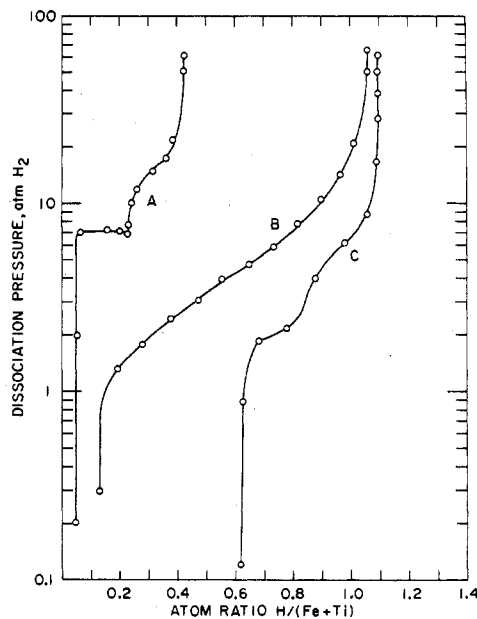


Figure 5. Pressure-composition isotherms for alloys of various Fe/Ti ratios at 40°: (A) 60.5 wt % Fe, 39.5 wt % Ti; (B) 50.5 wt % Fe, 49.2 wt % Ti; (C) 36.7 wt % Fe, 63.2 wt % Ti.

of over 3 upon increasing the nickel content of the alloy from LaNi<sub>4.90</sub> to LaNi<sub>5.5</sub>. Thus, in order to obtain reproducible behavior it is advisable to control the intermetallic composition as closely as possible. Upon increasing the Ti content to 63.2%, the pressure-composition isotherm C is greatly distorted as also shown in Figure 5. This alloy was annealed at 1000° for 12 hr and then quenched in an unsuccessful attempt to prepare metastable FeTi<sub>2</sub>; but only FeTi and Ti

(10) W. R. Pearson, "Handbook of Lattice Spacings and Structures of Metals," Vol. 2, Pergamon Press, London, 1967, p 242.

(11) K. H. J. Buschow and H. H. Van Mal, *J. Less-Common Metals*, 29, 203 (1972).

were produced. After hydriding, an X-ray diffraction pattern of the product indicated the presence of  $\text{FeTiH}_{\sim 2}$ ,  $\text{TiH}_{\sim 2}$ ,  $\text{FeTi}$ , and  $\text{Ti}$ . The increased amount of residual hydrogen in the solid is undoubtedly due to the presence of the stable titanium hydride.

Upon departing from the single-phase region in the opposite direction, *i.e.*, that of higher iron content, there appears to be no significant effect other than a reduction in the amount of hydrogen sorbed as shown in Figure 5. The starting alloy was a two-phase mixture,  $\text{Fe}_2\text{Ti}$  and  $\text{FeTi}$ , having an overall composition of 60.5 wt % Fe and 39.5 wt % Ti. The isotherm A is essentially congruent with that obtained with  $\text{FeTi}$ , indicating little interaction between the two

phases or solid solubility of Fe in  $\text{FeTi}$ ; an observation which is in accord with the known homogeneity range of  $\text{FeTi}$ . The amount of hydrogen actually sorbed is somewhat less than that expected from the proportionate amount of  $\text{FeTi}$  present in the alloy, which may be due to the mere physical presence of  $\text{Fe}_2\text{Ti}$ .

**Acknowledgment.** The authors wish to express their thanks to Messrs. J. Hughes and A. Holtz for their expert assistance in the laboratory.

**Registry No.**  $\text{FeTiH}$ , 39433-91-5;  $\text{FeTiH}_2$ , 39433-92-6; 37-70% Fe, 30-63% Ti, 39433-89-1;  $\text{H}_2$ , 1333-74-0;  $\text{FeTi}$ , 12023-04-0; Fe, 7439-89-6; Ti, 7440-32-6.

Contribution from the Department of Chemistry, University of Calabria, 87100 Cosenza, Italy, and the Institute of Organic Chemistry, University of Bologna, 40136 Bologna, Italy

## Reactivity of Mixed Carbonyl-Nitrosyl Complexes of Iron(0)

GIULIANO DOLCETTI,\* LUIGI BUSETTO, and ANTONIO PALAZZI

Received March 20, 1973

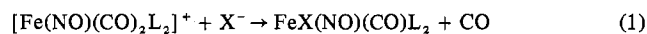
Neutral complexes of the type  $\text{FeX}(\text{NO})(\text{CO})\text{L}_2$  ( $\text{L} = (\text{P}(\text{C}_6\text{H}_5)_3)$  and  $\text{X} = \text{N}_3, \text{SCN}, \text{CNO}, \text{CN}, \text{SeCN}$ ;  $\text{L} = \text{P}(\text{CH}_3)(\text{C}_6\text{H}_5)_2$  and  $\text{X} = \text{N}_3, \text{SCN}$ ) have been prepared from the cationic  $[\text{Fe}(\text{NO})(\text{CO})_2\text{L}_2]^+$  complexes by reaction with the appropriate sodium salt. The formation of the azide complex  $\text{FeN}_3(\text{NO})(\text{CO})\text{L}_2$  from the starting carbonyl cationic complexes is related to the stabilization of a six-coordinate transition state due to the nitrosyl ligand. The geometrical configuration of the neutral complexes is discussed on the basis of the ir and nmr spectra.

### Introduction

The reactivity of nitrosyl complexes has recently received considerable attention.<sup>1</sup> The coordinated nitrosyl ligand has been found to be rather inert to displacement by electron-pair donors such as cyanide, hydroxide, and tertiary phosphines. This inertness to substitution is not found in the carbonyl case. Our interest in this field led us to study the reactivity of some cationic complexes in which both nitrosyl and carbonyl ligands are coordinated to the same metal.

### Results and Discussion

We now report the preparation and the characterization of a series of new compounds of the type  $\text{FeX}(\text{NO})(\text{CO})\text{L}_2$  ( $\text{L} = \text{P}(\text{C}_6\text{H}_5)_3$  and  $\text{X} = \text{N}_3, \text{SCN}, \text{CNO}, \text{CN}, \text{SeCN}$ ;  $\text{L} = \text{P}(\text{CH}_3)(\text{C}_6\text{H}_5)_2$  and  $\text{X} = \text{N}_3, \text{SCN}$ ). The compounds are obtained by reaction of  $[\text{Fe}(\text{NO})(\text{CO})_2\text{L}]^+\text{PF}_6^-$  recently reported by Johnson, *et al.*,<sup>2,3</sup> with the appropriate sodium salt.



From a 50:50 water-acetone suspension of dicarbonylnitrosylbis(tertiary phosphine)iron(0) a vigorous effervescence, with gas evolution, occurs after addition of the salt. The product spontaneously precipitates from the reaction mixture as a microcrystalline, colored solid.

\* To whom correspondence should be addressed at the Department of Chemistry, University of Calabria, 87100 Cosenza, Italy.

(1) J. P. Collman, N. W. Hoffman, and D. E. Morris, *J. Amer. Chem. Soc.*, **91**, 5659 (1969); (b) C. A. Reed and W. R. Roper, *J. Chem. Soc., Dalton Trans.*, 1243 (1972); (c) J. B. Godwin and T. J. Meyer, *Inorg. Chem.*, **10**, 471 (1971).

(2) B. F. G. Johnson and J. A. Segal, *J. Chem. Soc., Dalton Trans.*, 1268 (1972).

(3) B. F. G. Johnson and J. A. Segal, *J. Organometal. Chem.*, **31**, C79 (1971).

All the compounds are soluble in polar organic solvents such as acetone, acetonitrile, nitrobenzene, dichloromethane, and chloroform. However, they decompose rapidly in these solutions. For this reason it is essential to carry out the reactions in the presence of a large percentage of water to ensure rapid precipitation of the desired products, thus avoiding side reactions which lead to unidentified brown by-products. Reactions with  $\text{LiCl}$ ,  $\text{LiBr}$ , and  $\text{LiI}$  in acetone-water lead only to the metathetical exchange of the hexafluorophosphate anion by chloride, bromide, and iodide, since the ir spectra are identical with these of the starting materials.<sup>4</sup>

All the members of the series are stable to the air in the solid state for months. The nature of  $\text{FeX}(\text{NO})(\text{CO})\text{L}_2$  was established from elemental analyses (Table I), ir spectra, nmr spectra, and conductance measurements.

The ir spectra of the complexes (Table II) exhibit one  $\nu(\text{CO})$  stretching vibration in the range 1910–1930  $\text{cm}^{-1}$  and one  $\nu(\text{NO})$  stretching vibration in the range 1670–1700  $\text{cm}^{-1}$  consistent with the proposed formulation. The stretching vibrations for both the carbonyl and the nitrosyl groups are about 100  $\text{cm}^{-1}$  lower than these of the parent iron(0) complex. Although the two limiting coordination forms of the NO group,  $\text{NO}^+$  and  $\text{NO}^-$ , cannot be unequivocally distinguished on the basis of the  $\nu(\text{NO})$  frequency,<sup>5</sup> the appearance of the  $\nu(\text{NO})$  stretching vibration in the 1670–1700- $\text{cm}^{-1}$  range, for neutral complexes, suggests that the nitrosyl ligand is acting as a formal three-electron donor ( $\text{NO}^+$ ) and that the Fe–N–O arrangement is linear.

(4) G. R. Crooks and B. F. G. Johnson, *J. Chem. Soc. A*, 1238 (1968).

(5) G. Dolcetti, N. W. Hoffman, and J. P. Collman, *Inorg. Chim. Acta*, **6**, 531 (1972).